A Novel Ultra-fast High Resolution Time-domain EMI Measurement System based on Field Programmable Gate Arrays

Stephan Braun, Reinhard Schneider and Peter Russer

Munich University of Technology,
Institute for High-Frequency Engineering, Munich, Germany, stephan.braun@tum.de

Abstract — **Full Compliance Measurements of the electromagnetic interference (EMI) of electric and electronic devices in the past and now is performed with EMI Receivers operating in frequency-domain. Time-domain EMI Measurement Systems allow to reduce the measurement time by several orders of magnitude. In this paper we present a ultra-fast high resolution Time-domain EMI Measurement System that uses three analog-to-digital converters to digitize the signal with an improved dynamic range. Each analog-to-digital converter digitizes a part of the amplitude scale. By a field programmable Gate Array the signal of the three analog-to-digital converters is combined to a signal with high resolution. A novel algorithm to process a real valued signal with a complex DFT is presented. This algorithm allows to speed up to measurement by a factor of about 2000 in comparison to an EMI Receiver. In comparison to a conventional FFT algorithm the calculation time as well as the consumption of logic is reduced by a factor of 2. A further algorithm is shown that can calculate the spectrum with a smaller bin-width than a conventional FFT. By this algorithm an EMI measurement at any frequency independent of discretization given by the FFT in frequency-domain can be performed. The EMI signal of a device has been recorded with a novel multiresolution system that consists of several 10-Bit 2.3 GS/s analog-to-digital converters and processed by an implemented fast Fourier transform on Field Programmable Gate Arrays. The emission of a device under test has been investigated at 19600 discrete spectral values and 36 angles within 3 minutes. The results have been compared with results obtained by an EMI Receiver in the frequency range 30 MHz - 1 GHz.**

I. Introduction

Traditionally Measurements of the Electromagnetic Interference (EMI) are performed by EMI Receivers operating in frequency-domain. A drawback of such systems is the long measurement time up to several hours for a single frequency scan. For a complete EMI certification of a product measurements at several angles of the turntable have to be performed. Additionally the measurements have to performed with horizontal and vertical polarization and different elevations of the receiving antenna. In order to reduce the measurement time for frequency-domain measurements a measurement procedure has been presented [3] that consists of a pre-scan in the peak detector mode at a single position of the device under test (DUT) and final measurements at frequencies where the magnitude of the spectrum has been during the pre-scan over a certain threshold level. During each final measurement the maximum emission in dependence to the angle of the DUT and the height of the antenna is determined. A drawback of this procedure is that the emissions are only measured at the frequencies that have been during the pre-scan over a certain threshold level. Due to strong directivity of radiating sources or an insufficient long scan time during the pre-scan not all emission may have been detected. A possibility to solve this problem is to increase the scan time, which may result in a pre-scan time of several hours for instable radiating devices.

An efficient way to reduce the measurement time without reducing the number of measured discrete frequency values is the use of a time-domain EMI measurement system that uses the fast Fourier transform (FFT) and digital implementation of the detector modes to obtain the same result in a fraction of time than conventional EMI receivers. The system uses three analog-to-digital converters (ADCs) in parallel to obtain an improved dynamic range in comparison to a conventional ADC [2]. The block diagram of a Multiresoltion TDEMI Measurement System is shown in Fig. 1. The EMI signal is received

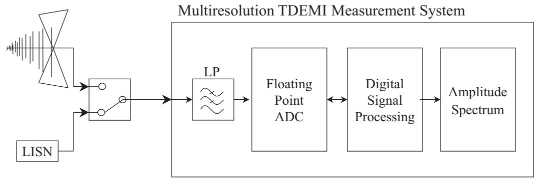

Fig. 1. Multiresolution Time-Domain EMI Measurement System

via a logarithmic periodic biconical antenna. By a multiresolution analog-to-digital converter (ADC) system a floating point analog-to-digital conversion is performed. The data is processed via digital signal processing and the amplitude spectrum is shown. An algorithm that allows to perform measurements under the peak, average and rms detector modes have been presented in [4]. In [1] it has been shown, that a Multiresolution TDEMI (MRTDEMI) measurement system can fulfill almost all requirements that are given by current international standards. In [5] it has been shown that such a system can be used to achieve compliance of products.

In the following we present a system that uses a Field Programmable Gate Array (FPGA) to process the signal via FFT. The system allows to reduce the measurement time by a factor of 2000 in comparison to conventional EMI receivers. By such a system an EMI measurement at each elevation of the antenna and each angle of the turntable can be performed in a shorter measurement time than a single scan at one elevation and angle with an EMI Receiver.

In order to reduce the hardware requirements we introduce a novel method that allows to increase the resolution of the DFT. By this method we can process a real valued input signal in half of the calculation time with half of the hardware resources. By performing a series of FFT calculations we can additionally increase the resolution in frequency-domain. By this way a measurement and detection at any frequency, independent of the bin-width of the DFT can be performed.

II. Discrete Fourier Transform

Digital spectral estimation is achieved via the Discrete Fourier Transform (DFT). Algorithms for DFT computations that exploit symmetry and repetition properties of the DFT are defined as Fast Fourier Transform (FFT). The DFT formulation considers periodic repetition of the time-domain signal and is given as follows:

$$X[k] = \sum_{n=0}^{N-1} x[n] e^{\frac{-j2\pi kn}{N}} \tag{1}$$

For FPGAs Intellectual Property (IP) cores that can perform the FFT within the microsecond range [6] are available. The number of samples per transform N is directly related to the sampling rate of the signal and the frequency bin-width by the following:

$$N = \frac{f_s}{\Delta f} \tag{2}$$

III. High Resolution FFT Algorithm

In the following we present a method that allows to calculate the spectrum of a real valued signal in time-domain with twice the resolution in frequency-domain by using the symmetry of the spectrum. Applying a complex window function on a real valued input signal leads to a complex output signal which is processed by a $\frac{N}{2}$ complex Fast Fourier Transform (FFT). After processing the signal with a $\frac{N}{2}$-FFT we obtain the even indexed frequencies in the first Nyquist zone and the odd indexed frequencies in the second Nyquist zone. By combining the frequencies of both Nyquist zones the complete spectrum is reconstructed.

The result of a Time Discrete Fourier Transform (TDFT) $Y(e^{jw})$ leads to a continuous spectrum which repeats periodic with $\omega = 2\pi$. Sampling the frequency-domain leads to a series $Y[k]$ with discrete frequencies $\omega_k = \frac{2\pi k}{N}$. This series is called Discrete Fourier-Transform (DFT) and is periodic to k and has N as a period.

$$Y[k] = Y(e^{j(\frac{2\pi k}{N})}) = Y(e^{j\omega})|_{\omega=\frac{2\pi k}{N}} \tag{3}$$

The discrete frequencies are given by:

$$f_k = k\frac{f_s}{N} = k\frac{1}{NT_s} \qquad 0 \le k \le N-1 \tag{4}$$

The product NT_s represents the observation time of the input signal and the length of the window function, respectively. The sampling rate is f_s the length of the DFT is N. The difference between two discrete frequencies f_k and f_{k+1} is calculated as $\frac{1}{NT_s}$. This corresponds to the inverse of the observation time of the input signal and is called bin-width $\triangle f$.

A. Symmetry of real series

Every real series $x[n]$ has a conjugated-symmetric Fourier-Transformed:

$$X(e^{j\omega}) = X^*(e^{-j\omega}) \tag{5}$$

The amplitude spectrum is symmetric:

$$|X(e^{j\omega})| = |X(e^{-j\omega})| \tag{6}$$

On the frequency axis the discrete frequency values from 0 to N represent the frequency-domain from 0 to the sampling frequency f_s as illustrated in Fig. 2 for $N = 16$. As a consequence of the symmetry of the amplitude spectrum, it is sufficient to regard the spectrum from 0 to $\frac{f_s}{2}$. This part of the spectrum is called first Nyquist zone. The second Nyquist zone on the frequency axis ranges from $k = \frac{N}{2}$ to N and contains the redundant information of the first Nyquist zone as it is symmetric.

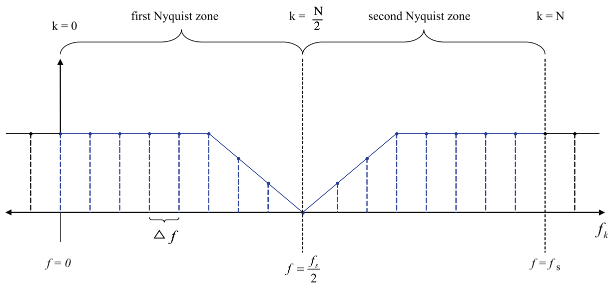

Fig. 2. Symmetric spectrum N=16

However, we can additionally gain information from the second Nyquist zone by sampling it at other frequencies than the first Nyquist zone. This can be realized by shifting the spectrum to lower frequencies by a factor of $0.25\triangle f$. In this case, the spectrum in the first Nyquist zone is sampled at frequency values which are located $0.25\triangle f$ higher than their original values, whereas the second Nyquist zone is sampled at frequencies located $0.75\triangle f$ higher than their original frequencies in the symmetric spectrum. In Fig. 3 the different distances of the first value in the first Nyquist zone f_0 and the first value in the second Nyquist zone f_{N-1} are illustrated for $N = 16$. Completing the first Nyquist zone with the odd

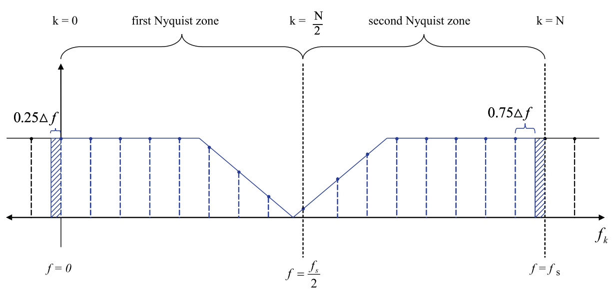

Fig. 3. Discrete frequency values f_k shifted by a quarter bin-width

indexed frequencies of the second Nyquist zone exactly halves the bin-width $\triangle f$ of the spectrum from 0 to $\frac{f_s}{2}$ as shown in Fig. 4.

As a consequence the frequencies of the second Nyquist zone can be used to complete the spectrum in the first Nyquist zone and increasing the spectral resolution by a factor of two as illustrated in Fig. 4.

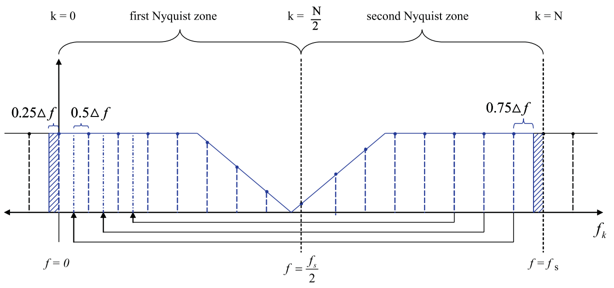

Fig. 4. Completion of the spectrum in the first Nyquist zone

B. Window function

In order to process a N-point FFT and avoid spectral leakage it is necessary to apply a window function $w[n]$ of length N on the input $x[n]$. As the window function of a TDEMI measurement system corresponds to the intermediate-frequency-filter (IF-filter) of a conventional EMI-Receiver in frequency-domain the frequency response of the window function has to be equal to the frequency response of the IF-filter. IF-filters implemented in EMI receivers usually provide a Gaussian frequency response. The used window function $w[n]$ is in time-domain as well as in the frequency-domain a Gaussian window. The window function is modelled in a way that in the frequency-domain the requirements given by CISPR 16-1-1 [7] are fulfilled.

C. Complex window function

A complex window function can be created by shifting a real valued window $w[n]$ in the frequency-domain. This leads to an asymmetric spectrum and results in a complex series in time domain. Mathematically, the shifting operation in frequency-domain corresponds to a phase rotation in time-domain:

$$e^{-j\omega_0 n}x[n] \longleftrightarrow X(e^{j(\omega+\omega_0)}) \tag{7}$$

The spectrum of a real valued Gaussian window is symmetric. In order to get a complex valued series in time-domain the window function has to be shifted in a way that the discrete frequency values k are shifted as presented in Fig. 3.

For the shifted window $w[n]_{shift}$ we obtain:

$$w[n]_{shift} = w[n]e^{-j\frac{2\pi n 0.25}{N}} \longleftrightarrow W[(k+0.25)\ mod\ N] \tag{8}$$

Fig. 5 shows an example of a complex Gaussian window shifted by $0.25\triangle f$ in frequency-domain. Windowing a real input series $x[n]$ with a complex window function $w[n]_{shift}$ results in a complex output series $z[n]$:

$$x[n]w[n]_{shift} = z[n] \tag{9}$$

A multiplication of an input series with a window in time-domain corresponds to a convolution of the input spectrum with the frequency response of the window function in frequency-domain.

$$x[n]w[n]_{shift} \longleftrightarrow X[k] * W[k]_{shift} \tag{10}$$

By this way the frequencies of the input spectrum are weighted with the frequencies of the window spectrum. As a result the output spectrum is calculated at the

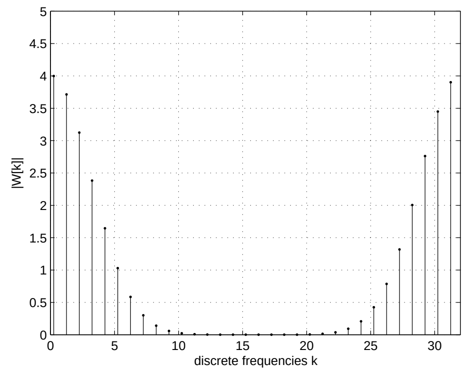

Fig. 5. 32-point Gaussian window shifted by L=0.25

shifted frequency values given by the complex window function. In time-domain the window function consists of an absolute value given by the real window function $w[n]$ and a phase $e^{-j\frac{2\pi n 0.25}{N}}$ which leads to a shifting of the signal by a quarter bin-width in frequency-domain as (8) indicates.

D. Processing of a real-valued N-point signal by a complex $\frac{N}{2}$-FFT

A complex Fast Fourier Transform (FFT) calculates N discrete frequencies $Z[k]$ from N complex input values $z[n]$. Using the presented method to complete the spectrum in the first Nyquist zone with the frequency values of the second Nyquist zone allows using a $\frac{N}{2}$-point complex FFT in order to evaluate a spectrum with N frequencies of a real valued signal.

Processing the FFT we use the Decimation-In-Frequency (DIF) algorithm [8]. DIF uses a $\frac{N}{2}$-DFT for calculating the even indexed frequencies $Z[k_{even}]$ of the output spectrum and another $\frac{N}{2}$-DFT to evaluate the odd indexed frequencies $Z[k_{odd}]$. As $Z[k_{odd}]$ is located between $Z[k_{even}]$ it is possible to derive these frequencies by using the symmetry of the input signal as described in III-A. Hence, it is sufficient to process a $\frac{N}{2}$-FFT to calculate the even frequency values $Z[k_{even}]$ only. It is therefore necessary to reduce the complex input series $z[n]$ to $\frac{N}{2}$ samples in order to process a $\frac{N}{2}$-FFT. As the DIF algorithm demands an addition of the

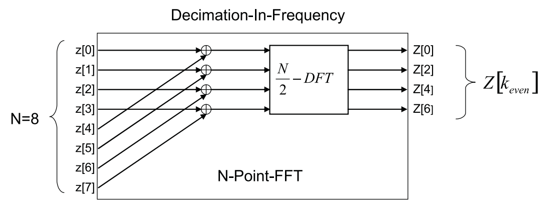

Fig. 6. DIF: calculation of $Z[k_{even}]$

first and the second half of the N input samples for calculating the even indexed frequencies of a N-point FFT as illustrated in Fig. 6 it is necessary to perform the complex addition before processing the $\frac{N}{2}$-FFT. Fig. 6 depicts the structure of the DIF algorithm for the calculation of the even indexed frequencies for a 8-point FFT. The result of the $\frac{N}{2}$-DFT block is an output spectrum

$Z[k_{even}]$ with $\frac{N}{2}$ frequency samples representing the even indexed frequencies of the N input samples of $z[n]$. The

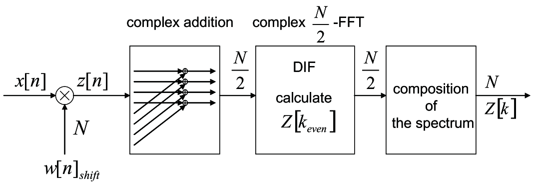

Fig. 7. System configuration

even indexed frequencies of the second Nyquist zone represent the odd frequencies of the first Nyquist zone. The frequencies of the second Nyquist zone are inserted between the two corresponding frequencies in the first Nyquist zone as illustrated in Fig. 4. By this way the odd indexed frequencies in the first Nyquist zone are derived and the spectrum is completed. Fig. 7 visualizes the different operations described in this section. As a result the spectral resolution of the $\frac{N}{2}$-FFT is doubled which leads to a spectrum with N discrete frequencies $Z[k]$.

E. Procedure to increase the number of discrete values

In the last chapter we have introduced a FFT algorithm that uses a complex window function in combination with a $\frac{N}{2}$ complex FFT to calculate the spectrum of the real valued EMI signal. We have introduced a factor $e^{\frac{-j2\pi ng}{N}}$ in time-domain which allows to move the signal in frequency-domain. As we have already seen we can shift the spectrum by any frequency. This shifting is independent of the bin-width given by the number of points of the FFT.

In order to increase the resolution of the FFT we need to perform several FFTs of the same signal and move the signal in frequency-domain by a multiplication with the factor $e^{\frac{-j2\pi ng}{N}}$.

To get a spectrum that has N' discrete spectral values we have to calculate a number of FFTs given by:

$$n_{FFTs} = \frac{N'}{N}. \tag{11}$$

The first FFT is calculated with $g = 0.25$. The incrementing of g is described by:

$$g' = g + g_w \tag{12}$$

with

$$g_w = \frac{1}{2n_i}. \tag{13}$$

After each increment of g the spectrum is calculated and the detector modes are applied. The merging of the complete spectrum from the calculated spectra is finally performed.

F. Measurements at any frequency value

An advantage of EMI-Receiver operating in frequency domain is the possibility to measure the magnitude of the spectrum at any selectable frequency. TDEMI measurement systems have a discrete spectrum with a bin-width according to (2). The problem can be solved by a multiplication of the EMI signal in time-domain with $e^{\frac{-j2\pi ng}{N}}$. By this way the complete spectrum can be shifted by a selectable frequency until a frequency bin that is calculated by the DFT will appear at the selected frequency. By this way g has to be determined according to:

$$g = f_d - f_b. \tag{14}$$

where f_d is the desired frequency and f_b is the nearest calculated spectral value by the DFT.

IV. Detector Modes

In a TDEMI measurement system in the frequency range 30 MHz - 1 GHz the sampling rate of the ADC has to be more than 2 GS/s to fulfill the Nyquist criterium. However FFT engines on FPGAs provide only a maximum clocking frequency of about 250 MS/s. We have shown that the data rate could be increased up to about 500 MS/s in section III-D. But by this way a continuous processing via a direct connection between the ADC and the FFT engine is still not possible. But for the statistical detector modes Peak, Average and RMS a continuous processing is from the mathematical point of view not necessary [4]. The signal can be stored temporarily and processed afterwards. With each calculation of the FFT the current spectrum can be updated.

The peak detector formulation is obtained by:

$$X_p = MAX\{X[n]|n \in \{1...N\}\} \tag{15}$$

The formulation of the average detector is given by:

$$X_{avg} = \frac{1}{N}\sum_{n=0}^{N-1} X[n] \tag{16}$$

The formulation of the rms detector is given by:

$$X_{rms} = \sqrt{\frac{1}{N}\sum_{n=0}^{N-1} X^2[n]} \tag{17}$$

V. Estimated Measurement Time

Table I outlines a comparison of the measurement time between the TDEMI system on FPGAs and EMI Receivers for a scan time of 100 ms in Band C and D. The result is a reduction of the measurement time by a factor about 2000.

	Realtime TDEMI	EMI Receiver
A/D Conversion	100 ms	-
Calculation time approx.	400 ms	-
Measurement time	< 1 s	33 min

TABLE I
Comparison of the measurement time

VI. Simulations and Measurement Results

In order to evaluate the FPGA based TDEMI measurement system we performed a measurement of the emission of a laptop and compared with the results obtained with an EMI receiver. The result is shown in Fig. 8. The maximum difference is 2 dB. The measurement time for the scan with the EMI Receiver has been several seconds. The measurement time with the TDEMI system that uses an implemented hardware FFT implementation has been below 1 ms.

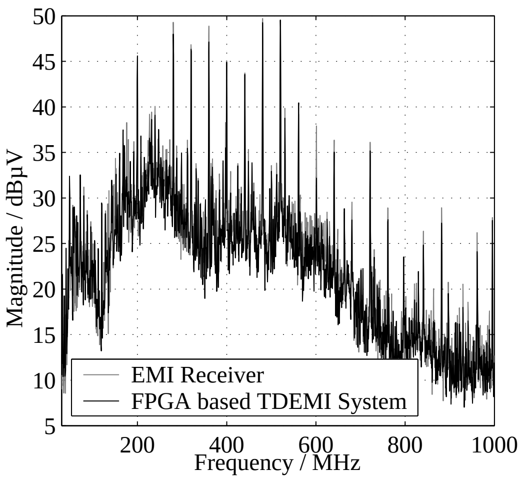

Fig. 8. Comparison EMI Receiver and FPGA based TDEMI System

In a further measurement the radiation of a Desktop Computer has been investigated. We performed a measurement at 36 radiation angles of the device under test. The scan time has been 5 ms. In Fig. 9 the amplitude spectrum in the average detector mode is shown. It is

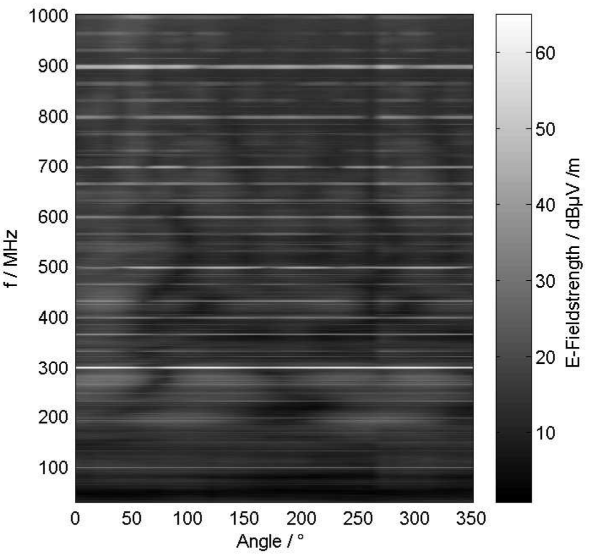

Fig. 9. Azimuth Scan of Desktop Computer (Case opened)

shown that the radiation at the fundamental clocking frequency of 300 MHz is almost independent of the angle. Other emissions e.g. at 800 MHz show minima and maxima over the complete azimuth scan. The difference between the minimum and the maximum is in this case more than 30 dB. Due to this strong dependence of the angle of the DUT it is not assured that during a conventional pre-scan the emission at this frequency is always detected.

VII. Conclusion

We have shown that a hardware implementation of the FFT can reduce the measurement time by a factor of 2000 in comparison to conventional EMI Receiver. By this way it is possible to perform an EMI measurement at all angles of the DUT and elevations of the antenna. By this way warranty is given that all frequencies have been investigated, but still the measurement time is reduced in comparison to a measurement the performs a pre-scan and a final scan. By this way pre-scans will become obsolete, because time-domain EMI measurements will give more accurate results in a shorter measurement time. Measurements at single frequencies will be possible independent of the bin-width of the used DFT.

VIII. Outlook

In this paper we have shown that results can be obtained for the peak, average and rms detector mode by using a hardware FFT. One of the next steps will be the implementation of the quasi-peak detector and to show that all requirements that are given by CISPR 16-1-1 can be fulfilled by such a system.

References

[1] S. Braun, M. Aidam, and P. Russer, "Development of a multiresolution time-domain emi measurement system that fulfils cispr 16-1," in *2005 IEEE International Symposium On Electromagnetic Compatibility, Chicago, USA*, pp. 388–393, 2005.

[2] S. Braun and P. Russer, "A low-noise multiresolution high-dynamic ultra-broad-band time-domain emi measurement system," *IEEE Transactions on Microwave Theory and Techniques*, vol. 53, pp. 3354–3363, Nov 2005.

[3] M. Stecher, "Automated measurement of emissions from equipment and systems," in *2002 IEEE International Symposium On Electromagnetic Compatibility Digest, August 19–23, Minneapolis, USA*, pp. 593–598, 2002.

[4] F. Krug, T. Hermann, and P. Russer, "Signal Processing Strategies with the TDEMI Measurement System," *2003 IEEE Instrumation and Measurement Technology Conference Proceeding, May 20–22, Vail, USA*, pp. 832–837, 2003.

[5] S. Braun and P. Russer, "Time-domain emi measurements performed with a multi-resolution system for product development and compliance," *The International Journal of Electromagnetic Compatibility*, vol. EMC Test and Design Guide 2005, pp. 18–26, Nov 2005.

[6] XILINX, *Fast Fourier Transform v3.1*. Data sheet, November 2004.

[7] CISPR16-1-1, *Specification for radio disturbance and immunity measuring apparatus and methods Part 1-1: Radio disturbance and immunity measuring apparatus – Measuring apparatus*. International Electrotechnical Commission, 2003.

[8] A. V. Oppenheim and R. W. Schafer, *Discrete–Time Signal Processing*. ISBN 0-13-214107-8, Prentice-Hall, 1999.